IEEE Access
Multidisciplinary | Rapid Review | Open Access Journal

Received October 2, 2018, accepted October 22, 2018, date of publication November 2, 2018, date of current version December 3, 2018.

Digital Object Identifier 10.1109/ACCESS.2018.2879372

A Physical Model of the Intracranial System for the Study of the Mechanisms of the Cerebral Blood Flow Autoregulation

ANTONIO FICOLA[1], MARIO LUCA FRAVOLINI[1], AND CARMELO ANILE[2]
[1]Department of Engineering, University of Perugia, 06123 Perugia, Italy
[2]Fondazione Policlinico Universitario A. Gemelli IRCCS–Università Cattolica del Sacro Cuore, 00168 Rome, Italy

Corresponding author: Antonio Ficola (antonio.ficola@unipg.it)

This work was supported in part by the Italian Ministero Università e Ricerca Scientifica PRIN 2008.

ABSTRACT This paper introduces a novel physical model of the intracranial system, which was built with the specific purpose of gaining a better insight into the fundamental mechanisms involved in the cerebral circulation. Specifically, the phenomena of passive autoregulation of the blood flow and the variation of the intracranial compliance as a function of the mean intracranial pressure have been investigated. The physical model allows to go beyond state-of-the-art mathematical models that are often based on strong assumptions or simplifications on the physical mechanisms governing the cerebral circulation. Indeed, the physical model based on passive components was able to correctly replicate some fundamental mechanisms of the blood flow autoregulation. In particular, it allows to highlight the role of the venous outflow, which behaves as a Starling resistor. The physical model can be employed as a demonstrator for educational purpose and to test the behavior of shunts for the therapy of hydrocephalus.

INDEX TERMS Intracranial system, physical model, passive autoregulation, intracranial compliance, Starling resistor.

I. INTRODUCTION

Modeling the intracranial system is an issue that was studied by a large number of authors. Lumped parameters models that consider only the main mechanisms have been introduced in several papers, as in: [1]–[6]. More detailed models of the intracranial circulation have been developed in [7]–[9], while a description of the cranial venous system can be found in [10]. Distributed parameters models of the arterial system have been developed and analyzed in [12] and [13]. Finally, a review and classification of state-of-the-art simulation models of the intracranial system can be found in [11].

Some of the above models consider the important mechanism of autoregulation. Autoregulation consists in ''constant blood flow through tissues whatever may be the height of general blood pressure'' [12]–[14]; it has been demonstrated to occur in several tissues and organs and is related to the adaptation of the vascular hydraulic resistance. Autoregulation mechanisms are typically divided in two broad categories: myogenic and hydraulic [3]–[5], [15]. Myogenic autoregulation is caused by different mechanisms [12], [16]; it is actuated by the smooth muscles of the arteries and takes some time to become fully effective; relevant mathematical models were developed for instance in [3]–[5], [15], and [17]. On the other hand, hydraulic regulation occurs in passive tubes and is characterized by a fast reaction to external disturbances (such as blood pressure). In particular, the main components are: an encapsulated system and soft-walled (namely, high compliant) tubes [12]. This behaviour occurs typically in the intracranial system, where arteries and veins are constrained inside the skull; for instance, in [15] myogenic autoregulation is assigned to arteries and arterioles that have smooth muscles, while the hydraulic regulation to the venous outflow, which consists of passive vessels.

The purpose of this paper is to present the results of specific experimental studies dealing with hydraulic autoregulation by means of a phantom model (in-vitro) of the intracranial system.

Specifically, the main contribution is to shown how the proposed physical (phantom) model is able to replicate some fundamental mechanisms of the intracranial system as the passive autoregulation and the dependency of the intracranial compliance on the intracranial pressure.

These phenomena have been investigated paying particular attention to the influence of the venous outlet, which is known to be a fundamental component on intracranial system.

The paper is organized as follows. Section II describes the phantom model and its subsystems, their design, the components selection and their assembly. Section III describes the experimental results and includes an analysis of the venous outlet. Section IV reports a the discussion of the experiments that show how some typical phenomena of the intracranial system can be replicated by means of purely passive hydraulic mechanisms. Finally, in section V some model limitations are pointed out.

II. MATERIAL AND METHODS

The physical model is composed of a container that mimics the skull, which encloses the cerebrovascular and ventricular subsystems, and the brain parenchyma. Fluids circulate and perfuse the different elements: blood, cerebrospinal fluid (CSF) and interstitial fluid [18]–[20].

The schemes of the physical model and of an electric circuit analogue representation are shown in Fig. 1. The fluid, which emulates the blood, is supplied by a controlled centrifugal pump and circulates through arteries, capillaries and veins; the fluid outflow takes place through the venous outlet in a reservoir at atmospheric pressure. Two pipes are employed to model the arteries; one of them is connected to the choroid plexus through a shunt. The veins circuit is implemented using two tubes that split into a number of smaller vessels, which mimic the venous outlet. The valves V1 and V2 are employed to regulate the fluid flow and the pressure drops, and to emulate the effect of arterioles and venules.

The cranial cavity is filled with the Cerebrospinal Fluid (CSF), which is produced and drained through the adjustable valves V3 and V4 that simulate the behaviour of the choroid plexuses and of the arachnoid villi, respectively.

The brain parenchyma (BP) compartment is perfused by the interstitial fluid, supplied by the capillary bed through valve V5.

It is possible to connect the CSF compartment to an external infusion pump to perform infusion tests, similar to those made in clinical practice. Pressures and flows are measured by a number of transducers. Some of them measure quantities that are not accessible ''in vivo'', namely distal arterial (AP), proximal venous (VP) and capillary pressures (CP), and are here employed to tune the model and to give a deep insight on the hydraulic response of the intracranial system.

The electric circuit analogy is a lumped parameter model, where it is put into evidence the fact that the hydraulic resistance of the venous outlet is not constant. In fact, all the parameters (resistances and compliances) are not constant in the physical system, because they depend on the pressures.

The 3D drawing of the model is shown in Fig. 2, while the actual physical model is shown in Fig. 3. The description of the different subsystems is given in the following paragraphs.

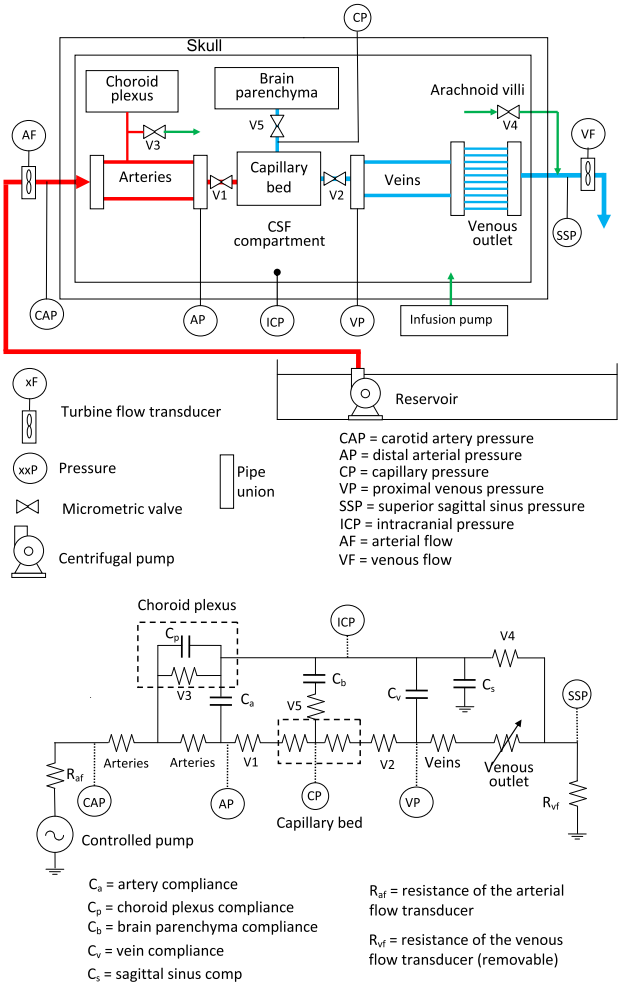

FIGURE 1. Scheme of the hydraulic circuit and of its electric circuit analogy.

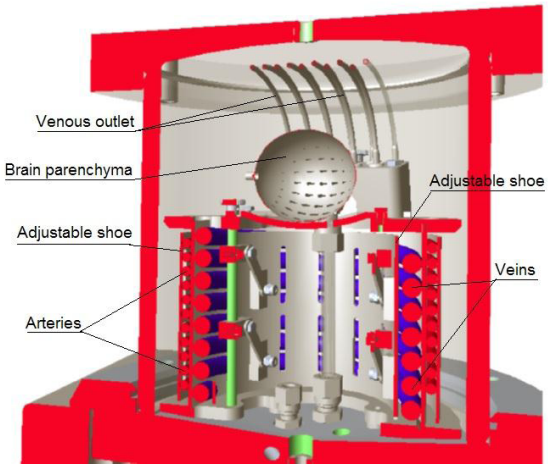

FIGURE 2. 3D drawing of the physical model with the main components.

A. THE CONTAINER

The container that emulates the skull is cylindrical (internal diameter × height = 145 mm × 150 mm); the base is made of stainless steel (20 mm thickness), the side wall is glass (9 mm

FIGURE 3. The physical model: the yellow balloon is used to model the interstitial volume and is connected to the capillary bed through valve V5 of Fig. 1.

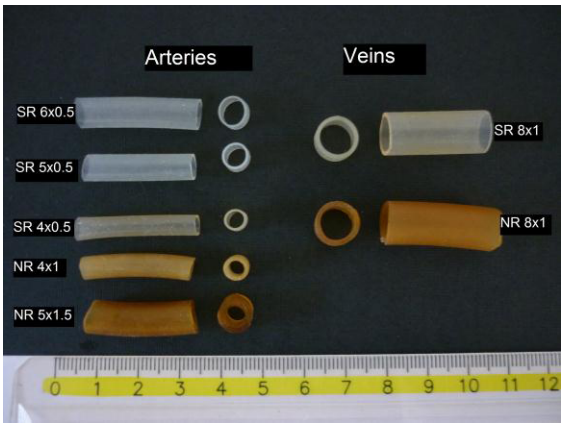

FIGURE 4. Pipes that have been employed as arteries and veins in the model (NR = natural rubber; SR = silicon rubber). Dimensions are internal diameter × thickness (mm).

thickness); the upper lid can be removed and is Plexiglas (thickness 20 mm).

B. FLUIDS

The fluid that emulates the blood can be composed of demineralized water or water/glycerol solutions to better simulate blood viscosity. In the latter case also the CSF would have the larger blood viscosity; this does not seem a relevant inconvenient, because the CSF flow (0.006 cm^3/s) is small compared to that of the blood (12.5 cm^3/s) [20]–[22]. In fact, a higher viscosity requires only the tuning of valves V3 and V4 to ensure the proper mean CSF pressure and flows.

C. ARTERIES AND VEINS

The arteries are emulated by means of two pipes to reproduce the right and left hemisphere circulations, as in the model of [8]; no distinction was made between carotid and vertebral arteries.

As for the venous circuit, it is particularly important to study the effect on the venous flow of the junction between the cortical bridging veins and the superior sagittal sinus [18]–[20]. For this purpose it was considered only the superior cerebral vein circuit that was modeled by two pipes. The venous outlet is described in a subsequent paragraph. The pressure drop caused by arterioles and venules is set-up by means of valves V1 and V2, respectively.

Arteries are wounded around a stainless cylinder; the veins are confined in the cylinder's interior, so that there is not a direct contact between them. Both arteries and veins are embraced by adjustable stainless steel shoes, employed to tune the vascular compliance (Fig. 2). If the shoes are loosened, the tubes can easily expand themselves in consequence of an increase of the transmural pressure (internal – external pressure); on the contrary, tightening the shoes makes the pipes more rigid. A number of different length, diameter, thickness and materials were tested to model different arteries and veins responses (Fig. 4).

D. CHOROID PLEXUS

Choroid plexuses are anatomical structures supplied by the choroidal arteries, which filter the arterial blood, producing the CSF. In consequence of their compliance, they pulsate as function of the arterial and intracranial pressures. In our demonstrator they are modeled by a Penrose tube, which implements the compliance and is inserted inside the cavity of the adjustable shoes of the veins, in order to prevent the direct contact with them. It is connected to one of the two arteries approximately in the midpoint. CSF production occurs through the micrometric valve V3. Different sizes were tested; the results reported in this study were obtained using a Penrose tube with diameter × length = 14 mm × 150 mm.

E. CAPILLARY BED

The capillary bed must guarantee the damping of the pulsatile component of the blood pressure jointly with a small pressure drop. It is not easy to replicate its anatomy and physiologic response. An attempt was made employing a hollow fiber oxygenator (Terumo Capiox® SX18-SX18R-SX25-SX25R), but only a poor damping was achieved, probably due to the small compliance of the polypropylene fibers. Therefore it was decided to employ an aluminium cylinder (internal diameter × height = 200 mm × 25 mm, wall thickness = 12 mm) filled with artificial sponges; suitable groves have been cut on the two bases to favor the spreading of the flow on the entire sponge surface (Fig. 5). These setup and materials were selected experimentally using a try-and-test procedure, with the goal of obtaining both the damping of the blood pulse pressure and a small pressure drop.

The blood is injected in the center of the lower base and drained at the upper base. In correspondence of the middle

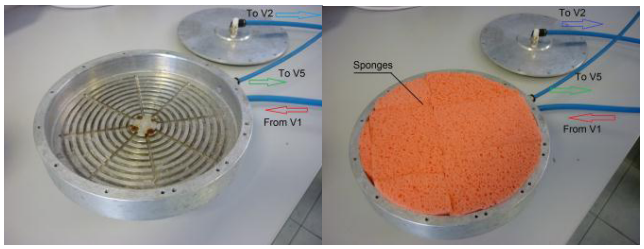

FIGURE 5. **The capillary bed. The left photo shows the container with the groves; the upper lid has the same groves. The right photo shows the artificial sponges. The capillary bed is connected to the circulatory system by means of the blue nylon pipes.**

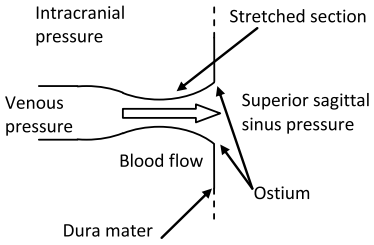

FIGURE 6. **Scheme of the sagittal section of a cortical bridging vein.**

cylinder height, a shunt is employed to supply the brain parenchyma with the interstitial fluid, filtered by valve V5; here, the capillary pressure sensor (CP) is connected.

F. BRAIN PARENCHYMA

Brain parenchyma (BP) behaves as a sponge for the interstitial fluid [23], [24], which originates from the capillary bed through the micrometric valve V5 (Fig. 1). The BP compliance is emulated using a natural rubber balloon (Figs. 2 and 3). Different volumes can be employed, with a maximum of 50 cm^3. It is possible to exclude the BP effects by closing valve V5.

G. VENOUS OUTLET

The venous outlet emulates the cortical bridging veins [18], [19], [20], [25]. An anatomic study of this structure is reported in [26]. It consists in about 10 – 15 veins, which collect the blood from the frontal and parietal lobes and carry it into the superior sagittal sinus, through a rigid ostium of the dura mater. One of these veins is schematized in Fig. 6 (see also [26]).

The vein cross section depends on the transmural pressure. Near the ostium, the intracranial pressure (ICP) is larger than in the superior sagittal sinus; therefore the vein tends to collapse, while the ostium remains open. Moving in the opposite direction of the blood flow, the internal pressure increases, reaching a value that makes the transmural pressure positive, so that the vein dilates.

From the hydraulic point of view, the venous outlet behaves like a Starling resistor, where the flow depends not only on the difference input-output pressure, but also on the external

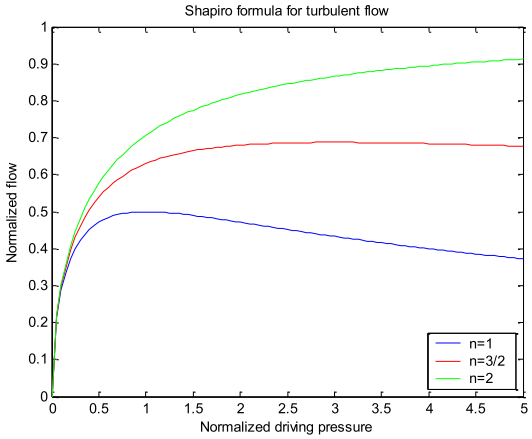

FIGURE 7. **Some Starling resistor characteristics as function of parameter *n*.**

one. This structure was investigated under constant pressure: analytically by [27], experimentally by [12] and [15]. The effect of ICP on the venous outlet was also investigated "in vivo" in rats by [25]. The case of unsteady flow has also been studied: numerical simulations in case of variable pressures were carried out in [28]–[31], while some experiments were carried out in [32]–[34].

In steady condition, the Starling resistor characteristics can be described by the following formula (see [27]), which was derived in case of highly compliant vessel:

$$\tilde{q}_{vo} = \frac{\tilde{p}_{ic}}{(1+\tilde{p}_{ic})^n} \tag{1}$$

where $\tilde{q}_{vo}$ is the nondimensional flow, $\tilde{p}_{ic}$ is the nondimensional driving pressure (namely the ICP, if the vessel is highly compliant), and n is a parameter that is chosen to fit experimental data (Fig. 7).

For small ICP the flow increases with the ICP itself. Depending on the value of exponent n, three situations may occur when ICP increases:

- $n > 3/2$, the flow always increases;
- $n = 3/2$, the flow tends to a constant value (autoregulation);
- $n < 3/2$, the flow tends to decrease.

In the last case the normalized differential hydraulic conductance $\tilde{G}_{vo} = d\tilde{q}_{vo}/d\tilde{p}_{ic}$ is negative. This gives rise to unstable steady solutions, where possible oscillations arise [28], [29], [35]. On these bases, heuristic formulae were proposed in [3]–[5] for the autoregulation mechanism. In these papers, the conductance of the Starling resistor is

$$G_{vo} = G'_{vo}\frac{p_v - p_{ic}}{p_v - p_{ss}} \tag{2}$$

where p_v, p_{ic}, p_{ss} are the venous, intracranial and superior sagittal sinus pressures, respectively. Since the blood driving pressure is $p_v - p_{ss}$, the venous outflow is

$$q_{vo} = p_v/G_{vo} = (p_v - p_{ic})/G'_{vo} \tag{3}$$

If the venous compliance is small, it is required that $p_v - p_{ic} > 0$ to avoid the collapse of venous bed; for the same reason $p_v - p_{ic}$ is almost constant and the flow is almost constant, thus achieving the condition "blood flow independent on the intracranial pressure" (autoregulation).

In the physical model, the venous outlet is composed of a maximum of ten pipes. We tested natural rubber (NR) Penrose tubes which are very compliant, and silicon rubber (SR) tubes which are much more rigid. SR tubes with a diameter of 4 mm and a thickness 0.5 mm collapse at pressures larger than 100 mmHg; SR tubes with smaller diameter and with the same thickness do not collapse at physiological pressure values. For these reasons, we employed more compliant tubes, namely 6 mm-width Penrose tubes (diameter 3.8 mm), which collapse with a negative transmural pressure of about 0.1 mmHg.

As for the instability phenomena, it was possible to induce oscillations using two Penrose tubes; in fact, the small number of pipes (two) makes the venous pressure (namely the driving pressure) large enough to generate undamped oscillations. On the other side, oscillations are not induced if more than four tubes are employed with a mean total flow of about 10 cm^3/s.

H. CSF SYSTEM

The central nervous system is completely surrounded by the cerebrospinal fluid, which also fills the inner cavities of the brain, namely the ventricles [18], [19]. The CSF system is composed of a production site (mainly the choroid plexuses) and an absorption district (mainly the arachnoid granulations from the subarachnoid space). In the present physical model there is not a distinction between ventricles and subarachnoid space. CSF production and absorption occur through two micrometric valves V3 and V4, which can be adjusted to have both the desired mean CSF flow (0.006 cm^3/s) and the mean ICP pressure (about 10-20 mmHg).

I. TUNING VALVES

The capillary bed communicates with arteries and veins through two micrometric valves V1 and V2 (Swagelok® Series L, flow coefficient Cv = 0.16). These valves are introduced to tune the mean pressure values of the arterial and venous districts. Valves V3, V4, and V5, which regulate the CSF and interstitial flows, are Swagelok® S-Series valves with flow coefficient Cv = 0.004.

J. SENSORS

Six Abbot Transpack® pressure sensors have been inserted to measure: the carotid artery pressure; the distal arterial, capillary and proximal venous pressures; the superior sagittal sinus and intracranial pressures (Fig.1). Arterial and venous flows are measured by two GEMS Ft-210® turbine flow rate sensors. Venous flowmeter causes an increase of the venous output pressure, namely the sagittal sinus pressure. This effect must be taken into account in the experiments and therefore the flowmeter must be temporary removed in case the physiological pressure values are considered. In any case, the sagittal sinus pressure is measured by the sensor SSP.

K. PUMP

A centrifugal submersible pump (25 W) was chosen to supply about 10-15 cm^3/s at a pressure of about 150 mmHg. The pump velocity (and its pressure/flow characteristic) is controlled by an inverter. It is possible to select different velocity profiles and frequencies in the range 48-80 beats/min. It is possible to connect the CSF circuit to a volumetric pump to carry out infusion tests.

L. DATA ACQUISITION

Data acquisition is performed by means of a Philips®CMS Patient Monitoring System M1167A with a sampling rate 1/128 s. To reduce the measurement noise, signals are post-processed using a third order type 2 Chebycheff low-pass filter with 30 Hz cutoff frequency. Signals are filtered forward and backward to prevent phase shift, thus preserving the original wave shape.

III. RESULTS

This section reports the results of a detailed experimental study, where a number of tests have been performed to evaluate the response of the physical model of the intracranial system under different operative conditions.

A. FIRST SET OF EXPERIMENTS

The purpose of these experiments is to show the different behaviour of the intracranial system with respect to other sites of the circulatory system. This was performed by measuring variables (signals) that are typically considered in the mathematical models but are not physically accessible in in-vivo experiments (for instance in [7]). We believe that the main differences originate from the fact that the intracranial circulatory system is confined in a closed space and the venous outlet ends abruptly in the superior sagittal sinus (Fig. 6). This produces a significant interaction between the arterial and the venous branches through the CSF. Conversely, in a not confined circulation, for instance in an arm, the ven circuit is practically decoupled from the arterial one, due to the presence of the capillaries that damp out any pulsation [21], [36].

The following configuration was employed in the experiments: SR arteries, internal diameter × thickness = 5 × 0.5 mm, length = 2 × 1.00 m; NR veins, internal diameter × thickness = 8 × 1 mm, length 2 × 1.0 m; venous outlet: ten Penrose tubes 6 mm-width, length 120 mm (long Starling resistors of Fig. 12). The arterial and venous blood volumes are therefore 40 cm^3 and 100 cm^3, respectively; these values are similar to those given in [7] and [8] and in the references therein reported.

The CAP replicates the internal carotid artery pressure. A sample of CAP trace is reported in [37]. To employ this signal in the physical model, we decided to measure the CAP on a human patient using the data acquisition system described in the section II-L. In Fig. 8 it is shown a sample of

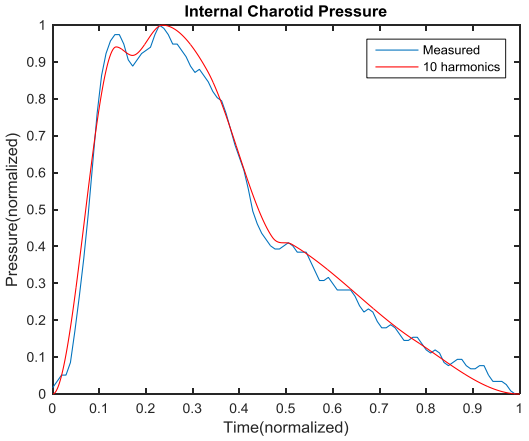

FIGURE 8. Normalized CAP used in the pump control system.

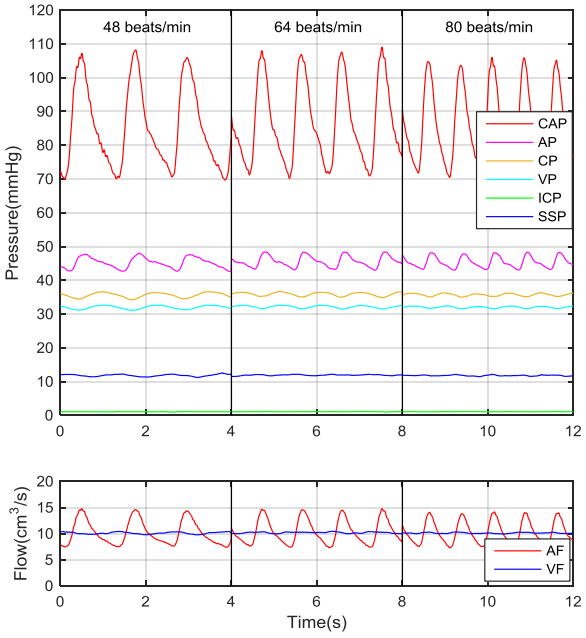

FIGURE 9. Pressures and flows in case of open skull.

a registered pressure signal and its approximation provided by ten harmonics of the Fourier series (in the figure pressure and time are normalized). The measured pressure waveform is similar to that reported in [37]. This signal was used as reference signal for the main pump velocity controller.

In a first test, the upper lid of the container was removed, as if the skull were open. The results of the experiment are shown in Fig. 9. In Table 1 the Fourier analysis of the different signals is reported; the standard deviation was 0.05 mmHg for the pressures (0.4 mmHg for the CAP), 0.1 cm^3/s for the flows and 2° for the phases. In this condition, only slight oscillations of the venous pressure have been observed; the 1st harmonic amplitude of the VP decreases as the frequency increases; the phase cannot be determined with adequate precision. The same occurs for the SSP and the VF, which are practically constant. Conversely the AP is marginally affected by the

TABLE 1. Harmonic analysis: open skull.

	Amplitude (mmHg)				Phase (°)		
48 bpm	Mean	1st	2nd	3rd	1st	2nd	3rd
CAP	86.1	16.5	7.5	2.1	0	-34	-55
AP	45.3	2.1	1.1	0.4	-41	-80	-126
CP	35.7	1.1	0.2		-136	143	
VP	32.0	0.7	0.1		-141	137	
SSP	11.8	0.4			138		
ICP	1.1						
AF	10.3	3.2	1.4	0.4	-3	-50	-72
VF	10.2	0.3	0.0	0.0	132	11	77
64 bpm	Mean	1st	2nd	3rd	1st	2nd	3rd
CAP	86.6	16.8	7.8	2.1	0	-33	-47
AP	45.4	2.1	1.3	0.5	-41	-97	-158
CP	35.7	0.7	0.1		-157	123	
VP	32.0	0.5			-165		
SSP	11.9	0.2			97		
ICP	1.1						
AF	10.4	3.3	1.5	0.4	-9	-55	-88
VF	10.3	0.2			85		
80 bpm	Mean	1 st	2nd	3rd	1st	2nd	3rd
CAP	86.4	16.8	7.6	2.4	0	-37	-48
AP	45.4	2.3	1.5	0.5	-44	-122	171
CP	35.7	0.6			-175		
VP	32.0	0.4			176		
SSP	11.8	0.1			63		
ICP	1.1						
AF	10.3	3.3	1.4	0.4	-15	-68	-103
VF	10.2	0.1			40		

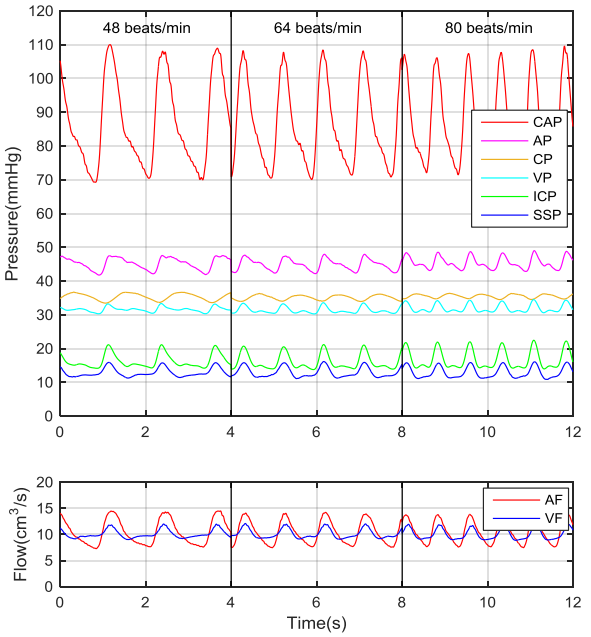

FIGURE 10. Pressures and flows in case of closed skull.

frequency and it is more similar to the CAP. In this case, the overall system behaves like a low-pass filter of the arterial pulse pressure.

TABLE 2. Harmonic analysis: closed skull.

	Amplitude (mmHg)				Phase (°)		
48 bpm	Mean	1st	2nd	3rd	1st	2nd	3rd
CAP	86.5	17.3	8.5	2.6	0	-36	-57
AP	45.1	2.3	1.1	0.6	-45	-68	-98
CP	35.3	1.5	0.3		-117	171	
VP	31.6	0.6	0.8	0.4	-19	-37	-84
SSP	12.9	1.6	1.1	0.4	36	-48	-105
ICP	16.3	2.3	1.9	0.9	11	-43	-89
AF	10.4	3.3	1.3	0.4	-8	-58	-78
VF	10.3	1.0	0.7	0.2	30	-69	-135
64 bpm	Mean	1st	2nd	3rd	1st	2nd	3rd
CAP	86.4	17.3	8.7	2.4	0	-37	-70
AP	45.0	2.1	1.5	0.7	-40	-73	-146
CP	35.1	1.1	0.2		-132	144	
VP	31.4	1.0	1.1	0.4	7	-56	-134
SSP	12.9	2.0	1.2	0.3	17	-76	-163
ICP	16.0	2.8	2.3	0.9	5	-62	-140
AF	10.4	3.2	1.2	0.4	-15	-59	-95
VF	10.3	1.3	0.7	0.2	6	-103	168
80 bpm	Mean	1 st	2nd	3rd	1st	2nd	3rd
CAP	86.4	17.7	8.5	2.3	0	-48	-67
AP	45.2	2.1	1.9	0.7	-34	-99	177
CP	35.5	0.8	0.2	0.0	-147	112	-8
VP	31.8	1.4	1.4	0.4	0	-93	-168
SSP	12.8	2.3	1.3	0.3	-5	-116	161
ICP	16.6	3.6	2.7	0.7	-1	-94	-174
AF	10.4	3.0	1.2	0.3	-22	-66	-101
VF	10.3	1.4	0.7	0.1	-21	-148	126

In a second test, the container was filled and closed. The results are reported in Fig. 10 and in Table 2. Venous and intracranial district signals (VP, SSP, ICP, VF) are characterized by an increase of the 1st and 2nd harmonic amplitudes with the increase of frequency, and a decrease of the corresponding phases. An exception is the 1st harmonic of the VP, which exhibits the opposite behavior of the phase; besides, in this case the 2nd harmonic is larger than the first one.

This behavior corresponds to the high frequency response of a notch filter (see Fig. 11), where the output amplitude increases and the phase decreases with the frequency as in region b), while the 1st harmonic of the VP falls as in region a). The different behavior of the various signals could be caused by the different values of the transmission zeros of the notch filter

$$F(s) = k\frac{\left(s^2 + 2\zeta\omega_n s + \omega_n^2\right)}{(s+p_1)(s+p_2)} \tag{4}$$

that depend on parameters k, ω_n, ζ, and determine the notch position, depth and width. Fitting a filter to the data is beyond the purpose of the experiment.

As final consideration it is worth mentioning that the significant phase variability as function of the frequency was also observed in in-vivo experiments made on pigs and described in [38]; in that paper the reference pressure was the femoral arterial one, while in the present study the reference is the carotid pressure (CAP).

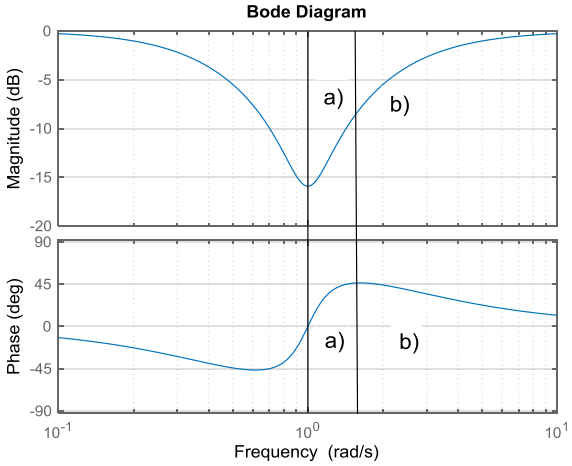

FIGURE 11. A sample of notch filter that can explain amplitude and phases of table 2: a) region with phase and amplitude increase; b) region with amplitude increase and phase decrease.

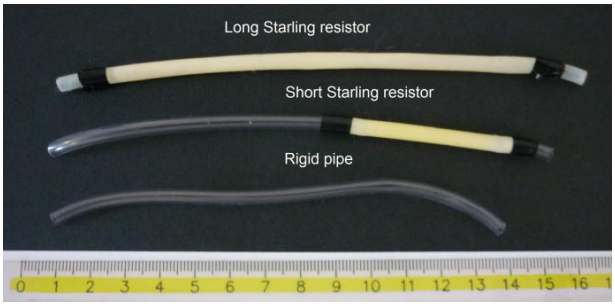

FIGURE 12. The different tubes employed in the experiments on the venous outlet.

B. SECOND SET OF EXPERIMENTS

The aim of these experiments was to show the effect of the venous outlet on the autoregulation mechanism.

Autoregulation consists in the fact that the mean blood flow remains constant despite variations of the mean arterial pressure or ICP. Assuming that the venous output pressure is zero, the driving pressure is the cerebral perfusion pressure (CPP), which is defined as CPP = CAP-ICP. In these experiments the mean CAP was kept constant while the ICP was increased by means an external infusion, which consists in injecting CSF at a proper rate by means of an infusion pump. In our tests, a flow rate of 1 cm^3/min was employed.

To investigate the effect of the venous outlet on this mechanism, we have carried out different experiments, using the setup of paragraph III-A, with three venous outlet configurations that consist in (see Fig. 12): ten 2 mm SR pipes (rigid outlet), ten 6 mm width Penrose tubes length 50 mm (short Starling resistors), and ten 6 mm width Penrose tubes length 120 mm (long Starling resistors).

During these tests it was employed a sinusoidal CAP at 64 beats/min. In order to better fit with the CPP definition, the venous flow sensor was removed because it causes an increase of the SSP. The CSF production and the absorption valves were tuned to generate a CSF flow of about

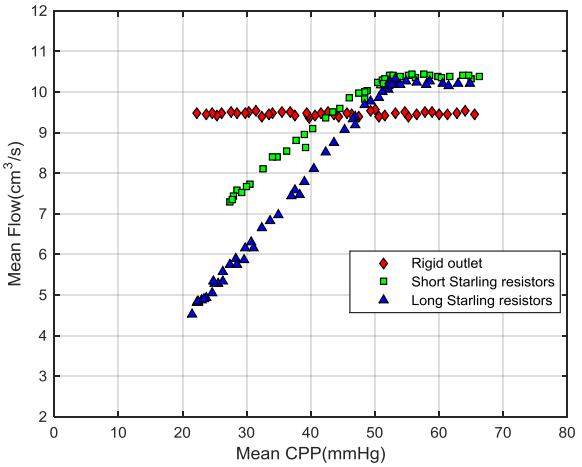

FIGURE 13. Autoregulation experiments: Arterial flow/CPP experimental characteristics during an infusion test with the three different venous outlet.

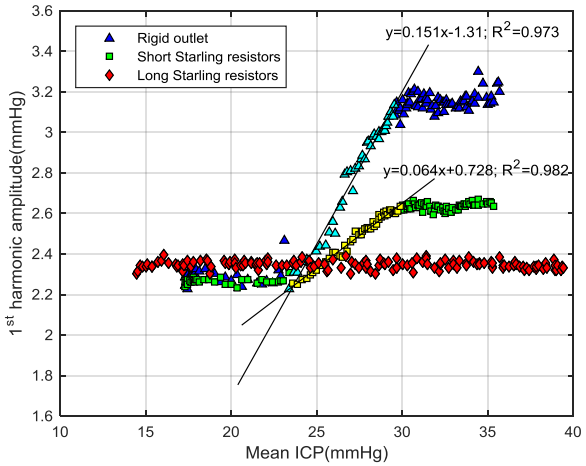

FIGURE 14. Infusion tests with different venous outlet. The linear regression was performed in the region where is relevant the effect of the compliance variation.

0.005 cm^3/s with 15 mmHg mean ICP; this mean flow was computed by considering the volume ejected through valve V4 in a two minutes period. The experimental results are reported in Fig. 13.

The observed behaviour is similar to the in-vivo experiments described for instance in [39]. Specifically, from the figure it can be clearly observed that the autoregulation mechanism is effective if the mean CPP does not fall below a certain critic value, beyond which the arterial flow AF decreases. In particular, autoregulation is lost when the mean CPP falls below about 50 mmHg in case of long and short Starling resistors. On the other side, in case of rigid pipes, no relevant effect is observed. In fact, in this case the CSF space and the vascular bed are practically independent; therefore the effect on the venous outlet is negligible, and reveals itself only at non physiological ICP values, when also the veins of the physical model tend to collapse.

C. THIRD SET OF EXPERIMENTS

The aim of these experiments is to show the effect of the venous outlet on the intracranial compliance during an infusion test [2], [40]–[44]. For these tests we employed the same setup of section III-B.

The results of the experiments are shown in Fig. 14, where linear regression between ICP mean value and the corresponding 1^{st} harmonic amplitude (AMP) is also shown. In case of rigid tubes, no significant relationship AMP/mean ICP was observed; conversely, in case of collapsible tubes, a proportional relationship AMP/ICP was observed (with slopes of +0.151 and +0.064 achieved through linear regression), depending on the effectiveness of the Starling resistors.

IV. DISCUSSION

The experiments have clearly shown that the proposed physical model is able to reproduce some fundamental mechanisms of the intracranial circulation. Specifically, we have proved that using only passive elements it is possible to reproduce phenomena such as the autoregulation and the variation of intracranial compliance as function of the mean intracranial pressure.

As for the passive autoregulation, the experiments confirm that this mechanism is strictly related to the Starling resistors at the venous outlet. We have experienced that the resistor nonlinearity is the main cause of the independence between the flow and the mean values of the perfusion pressure (CPP), if it is larger than a critic value. In this case an increase of the ICP (a decrease of the CPP) causes the closure of the venous outlet that, in turn, increases its hydraulic resistance. This would cause a reduction of the blood flow; but the higher hydraulic resistance gives rise to an increase of the venous pressure, which would cause a flow increase. The result is a feedback autoregulation of the flow that remains almost constant. In case the CPP is too small, the effect of the increase of the hydraulic resistance dominates, causing a reduction of the blood flow.

The variable compliance can also be explained by means of our implementation of the Starling resistors. In fact, for a specific value of the mean ICP, the pulse component tends to close the venous outlet, making the venous resistance ''instantaneously'' higher. Examining the electric circuit analogy of Fig. 1, these phenomena correspond to an abrupt increase of the output impedance, which causes a sudden increase of all the internal pressures. We can conclude that the higher the mean ICP is, the most effective the Starling resistor is. The upper breakpoint and plateau of the AMP/Mean ICP graph (Fig. 14) is caused by the compliance of the passive system that reaches a minimum; a further increase of the mean ICP would cause a flow reduction, as in Fig. 13. Finally, in case the Starling resistor pipes are shorter, they tend to behave as rigid pipes, because they are kept open by the increase of the venous pressure, as described in the autoregulation mechanism.

V. MODEL LIMITATIONS

The aim of the model is to show the effect of passive hydraulic elements on some mechanisms involved in the cerebral circulation. Therefore there are some simplifications that can be taken into account in evaluating the presented results.

- The arterial wall tension (which in human body is active) is not taken into account, as well as the effect of the arterial CO2 pressure on the reactivity of the cerebral vessels [3], [4] and on the cerebral blood flow.
- The mean intracranial pressure is artificially kept constant by valves V3 and V4 of Fig. 1, while the maintenance of the ICP within the physiological range is more complex in-vivo and still debated.
- The model compliance depends only on the vascular bed and the effect of human dural sinus rigidity is not considered.
- The brain parenchyma communicates only with the capillary bed; other possible pathways of the interstitial fluid have not been considered.

VI. CONCLUSIONS

In this paper it has been discussed the design and the experimentation of a phantom model of the intracranial circulation system. The prototype was designed with the specific purpose of validating and reproducing the fundamental physiological mechanisms that regulates the cerebral circulation. The experimental studies have indeed shown that the physical model can reproduce correctly the leading mechanisms of a real biological intracranial circulation system, in particular those involved in the passive autoregulation that depends strongly on the specific structure used to model the venous outlet. The capacity of the phantom of correctly emulating a physiological intracranial circulation response lays the foundations of its employment as a demonstrator for educational purposes and for testing possible strategies for the therapy of intracranial circulation pathologies, such as the hydrocephalus.

ACKNOWLEDGMENT

This work is dedicated to my (Anile) mentor, Harold Portnoy, MD.

The authors wish to tank Pietro Santini of the Fondazione Policlinico Universitario A. Gemelli IRCCS - Università Cattolica del Sacro Cuore, Rome, Italy for his support in data acquisition.

REFERENCES

[1] Z. M. Kadas, W. D. Lakin, J. Yu, and P. L. Penar, "A mathematical model of the intracranial system including autoregulation," *Neurol. Res.*, vol. 19, no. 4, pp. 441–450, 1997.

[2] M. Czosnyka *et al.*, "Contribution of mathematical modelling to the interpretation of bedside tests of cerebrovascular autoregulation," *J. Neurol. Neurosurg. Psychiatry*, vol. 63, no. 6, pp. 721–731, 1997.

[3] M. Ursino and C. A. Lodi, "Interaction among autoregulation, CO_2 reactivity, and intracranial pressure: A mathematical model," *Amer. J. Physiol. Heart Circulat. Physiol.*, vol. 274, no. 5, pp. 1715–1728, 1998.

[4] M. Ursino, A. T. Minassian, C. A. Lodi, and L. Beydon, "Cerebral hemodynamics during arterial and CO(2) pressure changes: *In vivo* prediction by a mathematical model," *Amer. J. Physiol. Heart Circulat. Physiol.*, vol. 279, no. 5, pp. H2439–H2455, 2000.

[5] M. Ursino and M. Giulioni, "Quantitative assessment of cerebral autoregulation from transcranial Doppler pulsatility: A computer simulation study," *Med. Eng. Phys.*, vol. 25, no. 8, pp. 655–666, 2003.

[6] M. Ursino and M. Giannessi, "A model of cerebrovascular reactivity including the circle of willis and cortical anastomoses," *Ann. Biomed. Eng.*, vol. 38, no. 3, pp. 955–974, 2010.

[7] M. Zagzoule and J.-P. Marc-Vergnes, "A global mathematical model of the cerebral circulation in man," *J. Biomech.*, vol. 19, no. 12, pp. 1015–1022, 1986.

[8] A. A. Linninger, M. Xenos, B. Sweetman, S. Ponkshe, X. Guo, and R. Penn, "A mathematical model of blood, cerebrospinal fluid and brain dynamics," *J. Math. Biol.*, vol. 59, no. 6, pp. 729–759, 2009.

[9] J. Ryu, X. Hu, and S. C. Shadden, "A coupled lumped-parameter and distributed network model for cerebral pulse-wave hemodynamics," *J. Biomech. Eng.*, vol. 137, no. 10, pp. 1–13, 2015.

[10] L. O. Müller and E. F. Toro, "Enhanced global mathematical model for studying cerebral venous blood flow," *J. Biomech.*, vol. 47, no. 13, pp. 3361–3372, 2014.

[11] W. Wakeland and B. Goldstein, "A review of physiological simulation models of intracranial pressure dynamics," *Comput. Biol. Med.*, vol. 38, no. 9, pp. 1024–1041, Sep. 2008.

[12] S. Rodbard, "Autoregulation in encapsulated, passive, soft-walled vessels," *Amer. Heart J.*, vol. 65, no. 5, pp. 648–655, 1963.

[13] W. M. Bayliss, "On the local reactions of the arterial wall to changes of internal pressure," *J. Physiol.*, vol. 28, no. 3, pp. 220–231, 1902.

[14] J. Kleinerman, S. M. Sancetta, and D. B. Hackel, "Effects of high spinal anesthesia on cerebral circulation and metabolism in man," *J. Clin. Invest.*, vol. 37, no. 2, pp. 285–293, 1958.

[15] H. D. Portnoy, M. Chopp, and C. Branch, "Hydraulic model of myogenic autoregulation and the cerebrovascular bed: The effects of altering systemic arterial pressure," *Neurosurgery*, vol. 13, no. 5, pp. 482–498, 1983.

[16] M. J. Davis, "Perspective: Physiological role(s) of the vascular myogenic response," *Microcirculation*, vol. 19, no. 2, pp. 99–114, 2012.

[17] S. Acosta, D. J. Penny, K. M. Brady, and C. G. Rusin, "An effective model of cerebrovascular pressure reactivity and blood flow autoregulation," *Microvascular Res.*, vol. 115, pp. 34–43, Jan. 2018.

[18] W. Kahle and M. Frotscher, *Color Atlas of Human Anatomy: Nervous System and Sensory Organs*. New York, NY, USA: Thieme, 2003.

[19] D. E. Haines, *Neuroanatomy: An Atlas of Structures, Sections, and Systems*, 6th ed. Baltimore, MD, USA: Williams & Wilkins, 2004.

[20] R. Rohkamm, *Color Atlas of Neurology*, 3rd ed. New York, NY, USA: Thieme, 2004.

[21] A. Guyton and J. Hall, *Textbook of Medical Physiology*, 11th ed. Philadelphia, PA, USA: Elsevier, 2000.

[22] L. Zarrinkoob, K. Ambarki, A. Wåring, R. Birgander, A. Eklund, and J. Malm, "Blood flow distribution in cerebral arteries," *J. Cerebral Blood Flow Metab.*, vol. 35, no. 4, pp. 648–654, 2015.

[23] S. Hakim, J. G. Venegas, and J. D. Burton, "The physics of the cranial cavity, hydrocephalus and normal pressure hydrocephalus: Mechanical interpretation and mathematical model," *Surg. Neurol.*, vol. 5, no. 3, pp. 187–210, 1976.

[24] R. D. Penn and J. W. Bacus, "The brain as a sponge: A computed tomographic look at Hakim's hypothesis," *Neurosurgery*, vol. 14, no. 6, pp. 670–675, 1984.

[25] L. M. Auer, N. Ishiyama, K. C. Hodde, R. Kleinert, and R. Pucher, "Effect of intracranial pressure on bridging veins in rats," *J. Neurosurg.*, vol. 67, no. 2, pp. 263–268, 1987.

[26] J.-R. Vignes, A. Dagain, J. Guérin, and D. Liguoro, "A hypothesis of cerebral venous system regulation based on a study of the junction between the cortical bridging veins and the superior sagittal sinus," *J. Neurosurg.*, vol. 107, no. 6, pp. 1205–1210, 2007.

[27] A. H. Shapiro, "Steady flow in collapsible tubes," *J. Biomech. Eng.*, vol. 99, no. 3, pp. 126–147, 1977.

[28] M. Heil, "Stokes flow in collapsible tubes: Computation and experiment," *J. Fluid Mech.*, vol. 353, pp. 285–312, Dec. 1997.

[29] X. Y. Luo and T. J. Pedley, "A numerical simulation of unsteady flow in a two-dimensional collapsible channel," *J. Fluid Mech.*, vol. 314, pp. 191–225, 1996.

[30] T. J. Pedley and X. Y. Luo, "Modelling flow and oscillations in collapsible tubes," *Theor. Comput. Fluid Dyn.*, vol. 10, nos. 1–4, pp. 277–294, Jan. 1998.

[31] X. Y. Luo, "Steady and unsteady flows in collapsible channels," in *Proc. Adv. Biomech.*, Beijing, China, Jun. 2001, pp. 192–199.

[32] R. D. Kamm and A. H. Shapiro, "Unsteady flow in a collapsible tube subjected to external pressure or body forces," *J. Fluid Mech.*, vol. 95, no. 1, pp. 1–78, 1979.
[33] S. K. Piechnik, M. Czosnyka, H. K. Richards, P. C. Whitfield, and J. D. Pickard, "Cerebral venous blood outflow: A theoretical model based on laboratory simulation," *Neurosurgery*, vol. 49, no. 5, pp. 1214–1223, Nov. 2001.
[34] A. I. Katz, Y. Chen, and A. H. Moreno, "Flow through a collapsible tube: Experimental analysis and mathematical model," *Biophys. J.*, vol. 9, no. 10, pp. 1261–1279, 1969.
[35] C. Cancelli and T. J. Pedley, "A separated-flow model for collapsible-tube oscillations," *J. Fluid Mech.*, vol. 157, pp. 375–404, Aug. 1985.
[36] A. Despopoulos and S. Silbernagl, *Color Atlas of Physiology*, 5th ed. New York, NY, USA: Thieme, 2003.
[37] P. Cole, P. Simpson, and G. B. Rushman, "Intra-arterial pressure monitoring: An alternative technique using winged needles," *Anaesthesia*, vol. 31, no. 1, pp. 69–72, 1976.
[38] C. D. Fraser, III, *et al.*, "The frequency response of cerebral autoregulation," *J. Appl. Physiol.*, vol. 115, no. 1, pp. 52–56, 2013.
[39] C. Zweifel, C. Dias, P. Smielewski, and M. Czosnyka, "Continuous time-domain monitoring of cerebral autoregulation in neurocritical care," *Med. Eng. Phys.*, vol. 36, no. 5, pp. 638–645, May 2014.
[40] C. J. J. Avezaat, J. H. M. van Eijndhoven, and D. J. Wyper, "Cerebrospinal fluid pulse pressure and intracranial volume-pressure relationships," *J. Neurol. Neurosurg. Psychiatry*, vol. 42, no. 8, pp. 687–700, 1979.
[41] S. Qvarlander, J. Malm, and A. Eklund, "CSF dynamic analysis of a predictive pulsatility-based infusion test for normal pressure hydrocephalus," *Med. Biol. Eng. Comput.*, vol. 52, no. 1, pp. 75–85, Jan. 2014.
[42] M. S. Daners, S. Bottan, L. Guzzella, D. Poulikakos, and V. Kurtcuoglu, "Craniospinal pressure–volume dynamics in phantom models," *IEEE Trans. Biomed. Eng.*, vol. 59, no. 12, pp. 3482–3490, Dec. 2012.
[43] J. D. Pickard and M. Czosnyka, "Management of raised intracranial pressure," *J. Neurol. Neurosurg. Psychiatry*, vol. 56, no. 8, pp. 845–858, 1993.
[44] M. Czosnyka, Z. Czosnyka, K. J. Agarwal-Harding, and J. D. Pickard, "Modeling of CSF dynamics: Legacy of professor Anthony Marmarou," in *Hydrocephalus* (Acta Neurochirurgica Supplementum), vol. 113. Berlin, Germany: Springer-Verlag, 2012, pp. 9–14.

ANTONIO FICOLA was born in Deruta, Italy, in 1957. He received the M.Sc. degree in mechanical engineering from the University of Rome, Italy, in 1982. From 1984 to 1986, he was at the University of Rome Tor Vergata in the field of flexible manufacturing systems. Since 1992, he has been a Research Assistant at the University of Perugia. His current research concerns robot control, modeling of biomedical systems, fault diagnosis, and control of unmanned aerial vehicles.

MARIO LUCA FRAVOLINI received the Ph.D. degree in electronic engineering from the University of Perugia, Perugia, Italy, in 2000. In 1999, he was with the Control Group, School of Aerospace Engineering, Georgia Institute of Technology, Atlanta, GA, USA. From 2000 to 2006, he was a Visiting Research Assistant Professor with the Department of Mechanical and Aerospace Engineering, West Virginia University, Morgantown, WV, USA. From 2005 to 2015, he was a Research Assistant with the Department of Engineering, University of Perugia, where he has been an Associate Professor of automatic controls since 2015. His current research interests include fault diagnosis, intelligent and adaptive control, predictive control, optical feedback, and active control of structures.

CARMELO ANILE was born in Santa Maria di Licodia, Catania, Italy, in 1950. He received the M.Sc. degree in medicine and surgery and the Specialist degree in neurosurgery from the Università Cattolica del Sacro Cuore, Rome, Italy, in 1974 and 1978, respectively. From 1980 to 2001, he was an Assistant Professor of neurosurgery with the Università Cattolica del Sacro Cuore, where he has been an Associate Professor in neurotraumatology with the Department of Neurosurgery since 2001. He has authored or co-authored about 160 papers in journals and congresses. His current research interests include brain tumors, brain vascular malformations, hypothalamus–pituitary pathology, head trauma, and epilepsy.